The Astrophysical Journal, 658:1349–1356, 2007 April 1

ELECTRONS AND PROTONS IN SOLAR ENERGETIC PARTICLE EVENTS

E. W. Cliver
Air Force Research Laboratory, Space Vehicles Directorate, Hanscom AFB, MA; edward.cliver@hanscom.af.mil

and

A. G. Ling
Atmospheric Environmental Research, Inc., Lexington, MA; alan.ling@hanscom.af.mil
Received 2006 June 19; accepted 2006 December 5

ABSTRACT

A plot of 0.5 MeV peak electron intensity versus >10 MeV peak proton intensity for well-connected solar energetic particle (SEP) events from 1997 to 2003 reveals two distinct populations: (1) a group of events with peak proton intensities <3 protons cm^{-2} s^{-1} sr^{-1} that have electron-to-proton (*e*/*p*) ratios ranging from $\sim 10^2$ to 2×10^4 and (2) a well-defined branch spanning peak proton intensities from ~3 to 10^4 protons cm^{-2} s^{-1} sr^{-1} with *e*/*p* ratios ranging from $\sim 10^1$ to 2×10^2. Events with strong abundance enhancements of trans-Fe elements form a prominent subset of "population 1" and are absent from "population 2." For a sample of poorly connected SEP events, population 1 largely disappears, and population 2 is observed to extend down to low ($<10^{-1}$ protons cm^{-2} s^{-1} sr^{-1}) proton intensities. Plots of 0.5 MeV peak electron intensity versus >30 MeV peak proton intensity yield comparable results. The SEP events in population 2 are highly (~90%) associated with dekametric/hectometric (DH) type II bursts versus only a ~20% association rate for population 1 events. Population 2 events have flatter electron (0.5–4.4 MeV) and proton spectra (10–30 MeV) than those in population 1. Based on their high *e*/*p* ratios, trans-Fe enhancements, poor association with DH type IIs, and inferred small "emission cones," population 1 events are attributed to acceleration in solar flares. For population 2 events, evidence for a dominant shock process includes their flatter spectra, apparent widespread sources, and high association with DH type II bursts.

Subject headings: acceleration of particles — shock waves — Sun: flares — Sun: particle emission

1. INTRODUCTION

Twenty years ago, papers by Klecker et al. (1984), Reames et al. (1985), Breneman & Stone (1985), and Mason et al. (1986) shifted the prime focus in studies of solar energetic particle (SEP) events from electrons and protons (e.g., Lin & Anderson 1967; Van Hollebeke et al. 1975; Lin & Hudson 1976; Lin et al. 1982; Cane et al. 1986) to the heavier ions, where it has remained since. Here we expand on an analysis from the earlier period to revisit the question of the acceleration mechanism for electrons and protons in large SEP events. In so doing, we have the advantage of modern SEP composition and solar radio measurements, and the motivation of a recent suggestion that shocks may be less important for particle acceleration in large SEP events than previously thought.

Our point of departure is the analysis from Ramaty et al. (1980), which is reproduced in Figure 1. Ramaty et al. interpreted the correlation between the peak intensities of 0.5–1.1 MeV electrons and 10 MeV protons, observed for proton events with peak intensities $>10^{-1}$ protons cm^{-2} s^{-1} sr^{-1} MeV^{-1}, in terms of a common acceleration process for the two species "closely related to the passage of shock waves through the solar atmosphere." They attributed the higher *e*/*p* ratios in smaller proton events to a high-energy tail of electrons from the first phase (flare) particle acceleration process. This picture, in which small SEP events dominated by electrons are linked to flares and type III bursts while larger events require shocks manifested by type II radio bursts, can be traced to Wild et al. (1963) and Lin (1970a). In broad terms, this is how matters have stood regarding particle acceleration at the Sun (see Reames 1999, for a comprehensive review) until a recent challenge posed by Cane and colleagues (Cane et al. 2002, 2003, 2006) based on low-frequency radio observations and SEP composition measurements. Specifically, Cane et al. (2003) argued that the flare acceleration process is generally dominant at >25 MeV $nucleon^{-1}$ ion energies in intense SEP events. This runs counter to the interpretation of Figure 1 and prompted us to redo the Ramaty et al. study for a larger sample of events and to extend the analysis to higher proton energies. In addition, we looked for differences in SEP spectra (for both electrons and protons) between events attributed to flares and those linked to shocks in our sample. Our analysis is presented in § 2, and the results are summarized and discussed in § 3.

2. ANALYSIS

2.1. *Event Selection, SEP Data Sources and Peak Intensities, and Database*

2.1.1. *Event Selection*

For our data sample, we used lists of SEP events compiled in the studies by Cane et al. (2002), Reames & Ng (2004), and Tylka et al. (2005). The Cane et al. list includes all measurable >20 MeV proton events detected by the Goddard SEP experiment on the *Interplanetary Monitoring Platform* (*IMP 8*) from 1997 January to 2001 May. We used the Reames & Ng (2004) table of large "impulsive" SEP events from 1994 November to 2003 September observed by the Low-Energy Matrix Telescope (von Rosenvinge et al. 1995) on the *Wind* spacecraft. A majority of the events on this list (25 of 39) exhibited strong enhancements of trans-Fe ions (by factors of 10^2–10^4 relative to coronal values, for $Z \geq 50$). From Tylka et al. (2005) we used the compilation of large SEP events from 1997 November to 2004 April; the sole criterion for event selection on the Tylka et al. list was a *Geostationary Operational Environmental Satellite* (*GOES*) >30 MeV event-integrated proton fluence $>2 \times 10^5$ protons cm^{-2} sr^{-1}. Through mid-2001, all events listed by Tylka et al. are

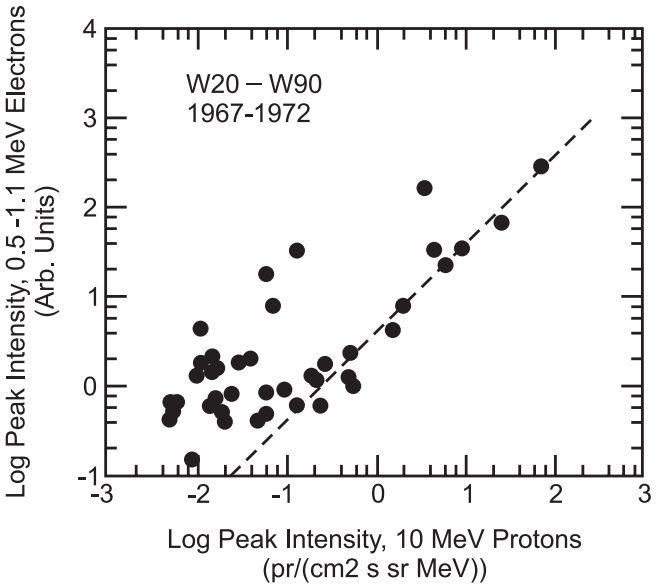

FIG. 1.— Plot of peak 0.5–1.1 MeV electron intensity vs. peak 10 MeV proton intensity for well-connected (W20°–W90°) SEP events from 1967 May to 1972 October (adapted from Ramaty et al. 1980).

included in the event table of Cane et al. In all there are 179 independent events on the three lists. We required flare locations for all events. Reames & Ng did not give source locations for their events, but Nitta et al. (2006) recently identified sources for 30 of them, and in each case the associated flare was well connected, located between W20° and W90° on the solar disk.[1] This is in accord with other results that indicate relatively narrow cones of emission for ^{3}He-rich and Fe-rich events (e.g., Reames et al. 1991; Wang et al. 2006). For all the other flares in our sample, we used the source locations indicated by Cane et al. (2002) and Tylka et al. (2005).

We subdivided the 179 events into three groups: 79 well-connected events (with associated flares from W20° to W90°), 34 west-limb events (with flare locations, suggested by Cane et al. [2002] from W91° to W150°), and 27 central meridian events (E40°–W19°). For symmetry, we did not consider events with associated flares east of E40°. Thus, the maximum range considered in either direction from the nominal "best-connection" longitude of W55° was 95°. This longitude restriction eliminated 13 events (all to the east). In addition, we eliminated 16 events for which Cane et al. listed a range of SEP times (e.g., 1998 April 29–May 2) rather than a single peak. Generally, these were complex events with long rise times originating in eastern hemisphere solar activity. We eliminated eight SEP events that lacked a reported flare and two events (1997 April 1 and 2002 July 15) with a delay of ~12 hr from flare to >10 MeV proton event onset. The final sample consisted of 140 events.

2.1.2. *SEP Data Sources and Peak Intensities*

For each of these 140 events, we determined hourly averaged peak intensities for >10 MeV protons, >30 MeV protons, 0.5 MeV electrons, and 4.4 MeV electrons. For proton data we used the *GOES* spacecraft (*GOES-8*, *-11*, and *-12*; in order of preference).[2] To check/augment these data we used >10 and >30 MeV proton data from the Solar Isotope Spectrometer (SIS; Stone et al. 1998) on the *Advanced Composition Explorer* (*ACE*).[3]

For electron data we used the 0.5 MeV (250–700 keV) and 4.4 MeV (2.64–6.18 MeV) channels from the Comprehensive Suprathermal and Energetic Particle Analyzer (COSTEP; Müller-Mellin et al. 1995) on the *Solar and Heliospheric Observatory* (*SOHO*). For periods when COSTEP data were unavailable, such as the extended *SOHO* outage during the second half of 1998, we used a correlation between *SOHO* 0.5 MeV electron peak intensities [I_{SOHO}(0.5 MeV)] and 175–315 keV electron peak intensities [I_{ACE}(250 keV)] from the Electron, Proton, and Alpha Monitor (EPAM) instrument (Gold et al. 1998) on *ACE* for well-connected (W20°–W90°) events, to calculate an equivalent COSTEP 0.5 MeV peak intensity (electrons cm^{-2} s^{-1} sr^{-1}):[4]

$$I_{SOHO}(0.5\ \mathrm{MeV}) = 5.47 I_{ACE}(250\ \mathrm{keV})^{1.08}; \quad r(\log) = 0.992. \tag{1}$$

We multiplied electron peak intensities by the channel bandwidth in each case for comparison with the peak integral proton intensities.

For both protons and electrons, our basic procedure was to select the largest peak occurring within ~12 hr of the 1–8 Å peak of the associated flare, thus restricting our focus to the prompt component of SEP events. (The ~12 hr window encompassed 17 events for which the selected >10 MeV proton peak was between 12 and 14 hr after the flare peak.) We subtracted the background intensity when the increase due to the identified solar event was less than a factor of 10 above the pre-event background (extrapolating any trends in the background intensity due to decay of preceding events to the time of the event peak). In most cases determination of the peak intensities was straightforward. Other events were more challenging, having either apparent multiple injections or extended profiles that peaked outside of the ~12 hr window. For events with multiple electron peaks, we picked the largest peak and the corresponding proton peak, subtracting backgrounds from earlier injections as required. For ~30 events with extended profiles, often complex, that peaked outside the ~12 hr window, we took the highest intensity within the interval. In the bulk of these events, subsequent peaks, exclusive of shock peaks, were less than a factor of 2 larger than the selected peak. In seven cases, however, later increases exceeded the selected peak by more than a factor of 2 (more on these events below). At low intensities, the *GOES* proton profiles are noisier than those observed by *ACE*, making it difficult to confidently identify peaks, even after visually smoothing the data. Thus, for nine small >10 MeV events and 19 small >30 MeV events, we used *ACE* peak intensity measurements to compute an equivalent *GOES* intensity from correlations (based on the W20°–W90° events in our data sample) between *GOES* and *ACE* >10 MeV peak intensities (protons cm^{-2} s^{-1} sr^{-1}),

$$I_{GOES}(>10\ \mathrm{MeV}) = 0.770 I_{ACE}(>10\ \mathrm{MeV})^{1.01}; \quad r(\log) = 0.992, \tag{2}$$

[1] The location for seven of the 30 events is given as W90°. These events are either at or within ~5° of the limb and were included in our well-connected subclass. Of the nine events without flare associations, six lacked images (two of these were attributed to flares at ≥W100° by Cane et al. [2002]), two had ambiguous sources, and one lacked both type III and imaged activity (N. Nitta 2006, private communication).

[2] See http://spidr.ngdc.noaa.gov/spidr/index.jsp.

[3] The galactic background is subtracted from the *GOES* data but not from the SIS data. The SIS proton data are available on the *ACE* Web site at http://www.srl.caltech.edu/ACE/ASC/browse/view_browse_data.html.

[4] Both the COSTEP and EPAM electron data are available on the Coordinated Data Analysis (CDA) Web site at http://cdaweb.gsfc.nasa.gov/cdaweb/istp_public/. COSTEP data for dates after 2002 January can be found at http://sohodata.nascom.nasa.gov/cgi-bin/gui.

TABLE 1

LIST OF EVENTS

FLARE				SEP EVENT			
	1–8 Å		LOCATION	ELECTRON INTENSITY[a]		PROTON INTENSITY[a]	
DATE[b]	Peak Time[c]	Intensity Class[d]	(deg)	0.5 MeV *SOHO*	4.4 MeV *SOHO*	>10 MeV *GOES*	>30 MeV *GOES*
1997 Apr 7	14:07	C6.8	S28E19	2.82e+01	3.68e−03	5.19e−01	8.38e−02
1997 May 12	04:55	C1.4	N21W07	6.93e+01	8.63e−03	7.85e−01	1.07e−01
1997 May 21	20:14	M1.3	N05W12	1.95e+02	2.25e−02	5.50e−02	3.76e−02
1997 Jul 25	20:34	C4.4	N16W54	1.52e+02	1.01e−02	2.83e−01	4.42e−02
1997 Sep 18*	00:00	B9.7	S25W76	9.83e+00	...	1.30e−01(A)	8.91e−02(A)
1997 Sep 18*	19:52	C1.5	S23W90	6.36e+00	2.08e−03	4.53e−02(A)	5.94e−02(A)
1997 Sep 24	02:48	M6.0	S31E19	3.02e+01	2.85e−02	1.60e−01	5.44e−02
1997 Oct 7	~13:20	...	W120	2.16e+01	3.21e−03	2.65e−01	6.04e−02
1997 Oct 21	17:53	C3.4	N16E07	7.88e+00	...	7.96e−02	1.67e−01(A)
1997 Nov 3	10:29	M4.2	S17W22	3.15e+01	3.03e−03	1.08e−01	3.76e−02
1997 Nov 4	05:58	X2.1	S14W33	6.52e+03	7.37e+00	5.48e+01	1.69e+01
1997 Nov 6	11:55	X9.4	S18W63	5.31e+04	1.15e+02	4.39e+02	1.79e+02
1997 Nov 13	21:15	...	W110	8.06e+02	9.59e−02	1.51e+00	2.04e−01
1997 Nov 14	~13:00	...	W120	1.36e+02	1.86e−02	4.67e−01	1.10e−01
1997 Dec 6	~12:40	...	N47W13	1.14e+00	...	5.93e−02	1.96e−01(A)
1998 Jan 26**	22:35	C5.5	S17W55	2.33e+02	9.24e−03	1.20e−01	3.70e−02
1998 Apr 20	10:21	M1.5	W90	1.40e+04	2.60e+01	3.40e+02	9.73e+01
1998 May 2	13:42	X1.2	S15W15	1.31e+04	8.38e+00	1.28e+02	4.13e+01
1998 May 6	08:09	X2.8	S11W65	4.64e+04	6.18e+01	1.42e+02	3.83e+01
1998 May 9	03:40	M7.7	W100	1.04e+03	5.81e−01	5.17e+00	1.38e+00
1998 May 27**	13:35	C7.6	N21W83	4.64e+02	2.16e−02	5.39e−02	2.91e−02
1998 May 30	22:50	...	W120	7.20e+01	5.69e−02	3.62e−02	1.98e−02
1998 Jun 16	18:39	M1.1	W115	9.90e+01	8.92e−03	1.23e+00	1.46e−01
1998 Aug 24	22:12	X1.1	N35E09	8.80e+03(A)	G	1.73e+02	2.73e+01
1998 Sep 6***	06:24	C2.8	W100	5.25e+01(A)	G	7.92e−01	1.55e−01
1998 Sep 9***	04:20	B9.9	W140	1.39e+03(A)	G	3.84e−01	6.94e−02
1998 Sep 23	07:12	M7.2	N19E09	2.05e+01(A)	G	5.60e−01	1.63e−01
1998 Sep 27*	08:08	C2.2	N21W48	2.12e+03(A)	G	2.35e−01	2.72e−02
1998 Sep 27*	23:38	C5.6	N20W58	8.22e+02(A)	G	4.01e−02	7.69e−02U
1998 Sep 29*	01:57	C6.0	N23W69	9.67e+01(A)	G	3.00e−02	8.41e−02U
1998 Sep 30	13:48	M3.0	N19W85	2.76e+04(A)	G	9.79e+02	1.12e+02
1998 Oct 18	21:05	...	W130	2.59e+03	3.42e−01	3.47e+00	4.04e−01
1998 Nov 14	05:18	C1.8	W120	3.80e+04	4.24e+01	2.87e+02	7.23e+01
1998 Nov 22	06:42	X4.1	S27W82	4.28e+01	2.11e−02	2.85e+00	9.02e−01
1998 Nov 24	02:20	X1.2	W108	3.95e+02	6.30e−01	9.61e−01	3.47e−01
1998 Dec 17	07:45	M3.4	S27W46	3.53e+01	3.40e−03	7.75e−02(A)	6.03e−02(A)
1999 Jan 3	15:09	C6.4	S23W49	5.83e+00(A)	G	1.44e−01	5.57e−02(A)
1999 Jan 7	00:06	C8.4	W95	1.74e+01(A)	G	9.22e−02(A)	3.47e−02(A)
1999 Feb 16	03:12	M3.4	S23W14	1.48e+01(A)	G	1.02e−01	2.94e−02
1999 Feb 20*	04:00	C8.2	S18W63	7.61e+00	2.25e−03	3.55e−02(A)	2.56e−02(A)
1999 Feb 20*	15:12	C3.6	S21W72	7.27e+00	...	1.67e−01U	9.84e−02U
1999 Apr 24	13:00	...	W150	4.26e+02	7.39e−02	2.85e+01	1.85e+00
1999 May 9	18:07	M8.4	W95	1.37e+02	8.81e−03	1.53e+00	2.27e−01
1999 May 27	10:45	...	W120	7.78e+02	3.15e−01	8.02e+00	1.23e+00
1999 Jun 1	19:03	C1.3	W120	1.57e+03	6.82e−01	3.48e+01	6.02e+00
1999 Jun 4	07:03	M4.2	N17W69	4.82e+03	7.62e−01	5.08e+01	2.80e+00
1999 Jun 11	~00:40	...	W120	3.61e+02	6.67e−02	3.56e+00	1.11e+00
1999 Jun 18*	11:29	B3.3	N25W90	4.10e+02	4.78e−02	7.55e−02	1.92e−02(A)
1999 Jun 27**	08:44	M1.1	N22W26	1.18e+02	1.04e−02	4.75e−02	1.09e−02
1999 Jul 25	13:36	M2.6	W95	1.85e+00	...	2.78e−02	2.47e−02
1999 Aug 7*	17:04	B1.7	N22W74	2.63e+00	...	1.64e−01U	9.78e−02U
1999 Aug 28	18:05	X1.2	S26W14	1.14e+01	3.98e−03	6.22e−02	2.54e−02
1999 Nov 17	09:57	M7.6	N17E21	1.66e+02(A)	G	1.75e−01	2.97e−02
1999 Dec 27*	01:48	M1.0	N24W35	1.05e+02	4.78e−03	2.54e−02(A)	9.65e−03(A)
1999 Dec 28**	00:48	M4.9	N20W56	1.41e+03	4.62e−01	1.39e−01	5.86e−02
2000 Jan 9	14:15	...	W120	2.86e+01	2.46e−02	6.70e−01	2.56e−02
2000 Jan 18	17:26	M4.0	S19E11	6.66e+01	1.56e−02	7.34e−01	2.64e−01
2000 Feb 12	04:10	M1.9	N26W24	7.65e+01	5.08e−03	1.62e+00	1.35e−01
2000 Feb 17	20:34	M1.4	S29E07	1.11e+02	2.22e−02	1.16e+00	2.32e−01
2000 Feb 18	09:27	C1.2	W120	2.32e+03	5.15e−01	1.15e+01	1.86e+00
2000 Mar 2**	08:28	X1.2	S14W52	3.06e+02	4.34e−02	2.15e−01	1.20e−01

TABLE 1—*Continued*

Flare				SEP Event			
	1–8 Å		Location	Electron Intensity[a]		Proton Intensity[a]	
Date[b]	Peak Time[c]	Intensity Class[d]	(deg)	0.5 MeV *SOHO*	4.4 MeV *SOHO*	>10 MeV *GOES*	>30 MeV *GOES*
2000 Mar 7*	12:28	C1.4	S15W72	5.19e+01	...	1.99e−02(A)	7.49e−03(A)
2000 Mar 7*	23:39	C3.5	S15W76	3.49e+01	...	2.69e−02	3.00e−02
2000 Mar 22	18:48	X1.2	N14W57	3.06e+01	3.12e−03	6.91e−01	6.23e−02
2000 Mar 24	07:52	X2.0	N15W82	1.08e+01	3.36e−03	5.00e−02	4.16e−02(A)
2000 Apr 4	15:39	M1.0	N16W66	5.22e+02	3.16e−02	3.17e+01	6.52e−01
2000 Apr 23	~12:25	...	W110	4.17e+01	2.27e−02	4.44e−01	1.81e−01
2000 Apr 27	~14:20	...	W120	2.71e+00	2.40e−03	1.17e−01	2.60e−02
2000 May 1*	10:21	M1.1	N21W50	1.60e+03	4.40e−02	1.85e−01	8.23e−02
2000 May 4*	11:00	C7.3	S17W90	3.85e+02	2.44e−01	8.91e−02	2.06e−02
2000 May 15	16:00	C8.2	S22W68	8.01e+02	1.70e−01	1.17e+00	5.12e−02
2000 May 23*	20:48	C7.3	N21W42	1.51e+02	2.29e−02	8.48e−02	1.91e−02(A)
2000 Jun 4*	07:02	B2.0	S10W62	1.27e+01	2.46e−03	1.42e−02(A)	1.37e−02(A)
2000 Jun 10	17:00	M5.6	N22W40	2.43e+03	1.78e+00	4.07e+01	1.02e+01
2000 Jun 15**	19:56	M2.0	N20W62	2.63e+02	1.33e−02	5.55e−02	3.03e−02
2000 Jun 17**	02:37	M3.9	N22W72	5.67e+02	1.13e−02	5.26e−01	6.81e−02
2000 Jun 18	01:59	X1.1	W95	6.29e+02	5.48e−02	2.62e+00	2.38e−01
2000 Jun 23**	14:31	M3.3	N23W72	1.37e+03	8.27e−02	1.15e+00	1.33e−01
2000 Jun 25	07:49	M2.1	N16W55	4.51e+01	1.04e−02	1.70e+00	6.86e−02
2000 Jun 28	19:10	C3.9	W95	2.13e+01	...	7.91e−02	2.25e−02(A)
2000 Jul 14	10:23	X6.1	N22W07	4.66e+05(A)	2.88e+03	7.94e+03	3.05e+03
2000 Jul 22	11:32	M3.9	N14W56	7.65e+02	1.58e−01	1.38e+01	3.36e+00
2000 Jul 27	~19:30	...	W120	4.70e+02	2.46e−02	8.20e+00	6.10e−01
2000 Aug 12*	12:30	B5.7	N05W48	2.77e+02	4.17e−03	4.77e−01	3.94e−02
2000 Sep 7	20:55	C7.7	N06W47	6.93e−01	...	1.60e−01	2.25e−02
2000 Sep 9	08:49	M1.7	N07W67	7.78e+01	...	3.60e−01	4.99e−02
2000 Sep 12	12:12	M1.0	S17W09	6.57e+03	1.27e+00	1.78e+02	7.86e+00
2000 Sep 16	04:26	M5.9	N14W07	3.25e+02	2.04e−02	2.72e+00	2.50e−01
2000 Sep 19	08:26	M5.1	N14W46	1.46e+02	7.58e−03	4.92e−01	4.22e−02
2000 Oct 16	07:35	M2.8	W95	4.28e+02	9.60e−02	1.33e+01	3.00e+00
2000 Oct 25	10:48	C4.0	W120	5.90e+02	8.91e−02	9.43e+00	7.75e−01
2000 Nov 8	23:27	M7.9	N10W75	2.45e+05	3.09e+03	1.15e+04	4.22e+03
2000 Nov 24	05:02	X2.2	N22W03	7.34e+02	1.36e−01	7.28e+00	2.01e+00
2000 Nov 24	15:13	X2.5	N22W07	9.94e+03	3.62e+00	7.66e+01	1.05e+01
2000 Dec 27*	23:40	B3.4	N13W36	6.73e+00	...	1.91e−02(A)	1.08e−02(A)
2000 Dec 28	12:05	C1.1	W150	1.33e+02	2.91e−02	3.18e−01	8.81e−02
2001 Jan 5	~16:50	...	W120	3.60e+02	2.36e−02	9.72e−01	1.29e−01
2001 Jan 28	15:58	M1.7	S04W59	2.01e+03	4.38e−01	2.78e+01	4.71e+00
2001 Feb 11	01:22	C7.0	N24W57	1.28e+02	5.47e−03	4.35e−01	5.38e−02
2001 Feb 26	05:05	...	W120	2.70e+02	1.01e−02	9.94e−01	5.57e−02
2001 Mar 10**	04:05	M7.3	N27W42	3.27e+02	1.34e−01	3.60e−02	2.38e−02
2001 Mar 29	10:15	X1.8	N16W12	3.63e+03	1.51e+00	2.55e+01	3.51e+00
2001 Apr 2	11:00	X1.5	N16W62	5.16e+02	4.57e−02	2.53e+00	5.42e−01
2001 Apr 2	21:50	X18.4	N17W78	3.41e+04	8.51e+01	6.59e+02	1.45e+02
2001 Apr 9	15:34	M8.5	S21W04	6.84e+02	8.93e−01	4.12e+00	1.82e+00
2001 Apr 10	05:26	X2.3	S23W09	2.02e+03	1.25e+00	7.89e+01	1.26e+01
2001 Apr 12	10:28	X2.2	S20W42	2.19e+03	2.48e+00	3.90e+01	1.20e+01
2001 Apr 14*	17:10	C3.9	S18W71	1.64e+03	3.27e−02	4.60e−01	6.67e−02
2001 Apr 15	13:50	X15.8	S20W84	6.21e+04	3.54e+02	9.00e+02	5.94e+02(A)
2001 Apr 18	02:14	C2.4	W120	6.11e+03	8.95e+00	2.03e+02	6.96e+01
2001 May 7	~08:55	...	W140	2.03e+02	2.91e−02	1.36e+01	1.79e−01
2001 May 20	06:03	M7.1	W120	7.16e+02	3.71e−01	6.16e+00	2.49e+00
2001 Aug 15	24:00	...	W140	4.36e+04	9.43e+01	3.64e+02	2.25e+02
2001 Sep 10*	13:22	B6.0	N18W90	1.29e+01	3.42e−03	2.50e−02	1.23e−02(A)
2001 Sep 11*	09:35	C8.3	N27W90	1.17e+01	2.40e−03	3.02e−02	1.37e−02(A)
2001 Sep 24	10:35	X2.7	S16E23	7.65e+04	2.87e+02	1.53e+03	4.34e+02
2001 Oct 1	05:15	M9.1	S20W88	7.32e+03	7.92e+00	1.46e+02	1.37e+01
2001 Oct 22	15:08	M7.0	S21E18	1.50e+03	1.26e+00	2.01e+01	4.06e+00
2001 Nov 4	16:19	X1.1	N06W18	1.27e+05	1.02e+03	2.99e+03	9.75e+02
2001 Nov 22	23:27	M4.1	S15W34	3.20e+04	2.81e+02	2.99e+03	5.55e+02
2001 Dec 26	05:36	M7.6	N08W54	2.79e+04	1.01e+02	7.24e+02	2.83e+02
2002 Apr 14*	22:25	C5.4	N18W75	3.53e+01	2.24e−03	1.20e−01	1.91e−02
2002 Apr 15*	02:45	C7.4	N20W79	1.22e+02	4.40e−03	9.19e−02	2.15e−02

TABLE 1—*Continued*

Flare				SEP Event			
	1–8 Å		Location	Electron Intensity[a]		Proton Intensity[a]	
Date[b]	Peak Time[c]	Intensity Class[d]	(deg)	0.5 MeV *SOHO*	4.4 MeV *SOHO*	>10 MeV *GOES*	>30 MeV *GOES*
2002 Apr 21	01:47	X1.7	S14W84	6.70e+04	3.16e+02	2.09e+03	6.34e+02
2002 May 22	03:48	C5.2	S22W53	2.02e+02	2.19e−02	6.77e+00	3.47e−01
2002 Aug 3*	19:05	X1.0	S16W80	1.28e+02	1.68e−02	1.88e−01	5.38e−02
2002 Aug 4*	14:52	C3.6	S13W90	1.10e+02	5.60e−03	9.34e−02	1.72e−02(A)
2002 Aug 18*	21:10	M2.2	S13W20	8.61e+02	4.55e−02	2.59e+00	3.12e−01
2002 Aug 19*	10:30	M2.1	S12W26	3.85e+03	1.44e−01	7.58e−01	6.70e−02
2002 Aug 19*	20:57	M3.1	S11W32	1.55e+03	2.35e−02	1.68e−01	3.30e−02
2002 Aug 20*	08:25	M3.4	S11W38	1.93e+04	1.51e+00	1.47e+00	2.71e−01
2002 Aug 22	01:57	M5.9	S07W62	1.90e+03	1.39e+00	3.13e+01	1.01e+01
2002 Aug 24	01:11	X3.5	S02W81	2.22e+04	3.34e+01	3.03e+02	1.17e+02
2002 Sep 27*	01:18	C4.2	S15W90	1.54e+03	4.99e−01	8.34e−02	1.29e−02
2002 Nov 9	13:23	M4.9	S12W29	6.00e+03	2.64e+00	2.14e+02	8.31e+00
2003 Oct 26	18:11	X1.4	N02W38	4.35e+04	4.30e+01	3.74e+02	3.64e+01
2003 Oct 28	11:10	X18.4	S16E08	5.72e+04	1.64e+03	8.28e+03	3.33e+03
2003 Oct 29	20:49	X10.8	S15W02	1.13e+05	8.98e+02	1.71e+03	6.63e+02
2003 Nov 2	17:25	X9.3	S14W56	6.26e+04	1.86e+02	1.31e+03	3.55e+02
2003 Nov 4	19:44	X18.4	S19W83	6.51e+03	6.69e+00	3.03e+02	4.93e+01

[a] Units = particles cm^{-2} s^{-1} sr^{-1}; . . . = not detectable above background; (A) = intensity derived from *ACE* measurement; G = data gap; U = upper limit.
[b] * = Well-connected impulsive event from Reames & Ng (2004); ** = impulsive SEP identification based on $e/p > 1000$; *** = poorly connected impulsive event from Reames & Ng (2004).
[c] For the 30 events from Reames & Ng (2004) with disk sources identified by Nitta el al. (2006), this time refers to the onset of DH type III emission. For all other events, the time is for the peak of the 1–8 Å burst unless the intensity class is . . . , in which case the time is the onset of DH type III emission taken from Cane et al. (2002).
[d] For the 30 events from Reames & Ng (2004) with disk sources identified by Nitta el al. (2006), the 1–8 Å intensity (with background intensity subtracted) was taken from Nitta et al. For all other events, no adjustment was made for the background.

and between *GOES* and *ACE* >30 MeV peak intensities,

$$I_{GOES}(>30\ \mathrm{MeV}) = 0.660 I_{ACE}(>30\ \mathrm{MeV})^{0.988};$$
$$r(\log) = 0.988. \quad (3)$$

For a few cases in which the electron/proton detectors on the primary (*SOHO*/*GOES*) spacecraft appeared to be saturated, peak intensities were calculated from observations on *ACE*.

2.1.3. *Database*

The dates, times, locations, and peak 1–8 Å intensities of the 140 solar events in our sample along with their associated peak particle intensities (with pre-event backgrounds subtracted) are given in Table 1.

2.2. *Electron versus Proton Scatter Plots*

2.2.1. 0.5 MeV *Electrons and* >10 MeV *Protons*

Our update of the Ramaty et al. (1980) analysis is given in Figure 2 (*top*). In this figure, the filled blue circles represent the Reames & Ng (2004) impulsive events, and filled black circles represent the Cane et al. (2002) and Tylka et al. (2005) events. It can be seen that the Reames & Ng events have small (<3 protons cm^{-2} s^{-1} sr^{-1}) peak proton intensities. The three least-squares lines drawn in the figure for peak proton intensities >3 protons cm^{-2} s^{-1} sr^{-1} represent two relations obtained by using either parameter in turn as the independent variable and a third (specified in the figure) obtained by taking the geometric mean of the resulting lines. Figure 2 (*top*), with the observed large scatter for small proton events and the well-defined branch for larger (>3 protons) peak >10 MeV intensities, closely resembles Figure 1. We refer to the small proton events as population 1 events, and those comprising the well-defined branch on the right of the figure as population 2. The *e*/*p* ratios of the population 1 events span a broad range of values, from $\sim 10^2$ to 2×10^4. The least-squares relationship between electron and proton intensities for population 2 events indicates a lower, and narrower, range of *e*/*p* values, from $\sim 10^1$ to 2×10^2.

Note that combining a large population 1 event and a large population 2 event will result in an event with an *e*/*p* ratio that falls in the range of population 2 events. This is true even after normalizing for flare size. Based on integrated flare soft X-ray intensity above the M1 level, the largest flares associated with population 1 events are approximately 2 orders of magnitude smaller than their population 2 counterparts.[5] If we take the population 1 event in Figure 2 (*top*) with the highest electron intensity, multiply its SEP electron and proton intensities by 100, and add them to the intensities of the largest population 2 event, the *e*/*p* ratio of the resulting event is ~200, within the characteristic range for population 2 events.

The enriched trans-Fe composition of many population 1 events, a characteristic attributed to the flare SEP acceleration mechanism (Reames 2000; Mason et al. 2004; Reames & Ng 2004), is consistent with the suggestion of Ramaty et al. (1980) that the high *e*/*p* ratios in the smaller proton events in Figure 1 result from particle acceleration in flares. An examination of the listing of *Wind* WAVES (Bougeret et al. 1995) dekametric/hectometric (DH) type II bursts compiled by M. Kaiser[6] for the large impulsive

[5] The largest flare associated with a population 1 event had an X1 1–8 Å peak intensity classification (2002 August 3; Leske et al. 2003; Nitta et al. 2006) vs. X28 for the largest population 2 event (2003 November 4).
[6] Available at http://lep694.gsfc.nasa.gov/waves/waves.html.

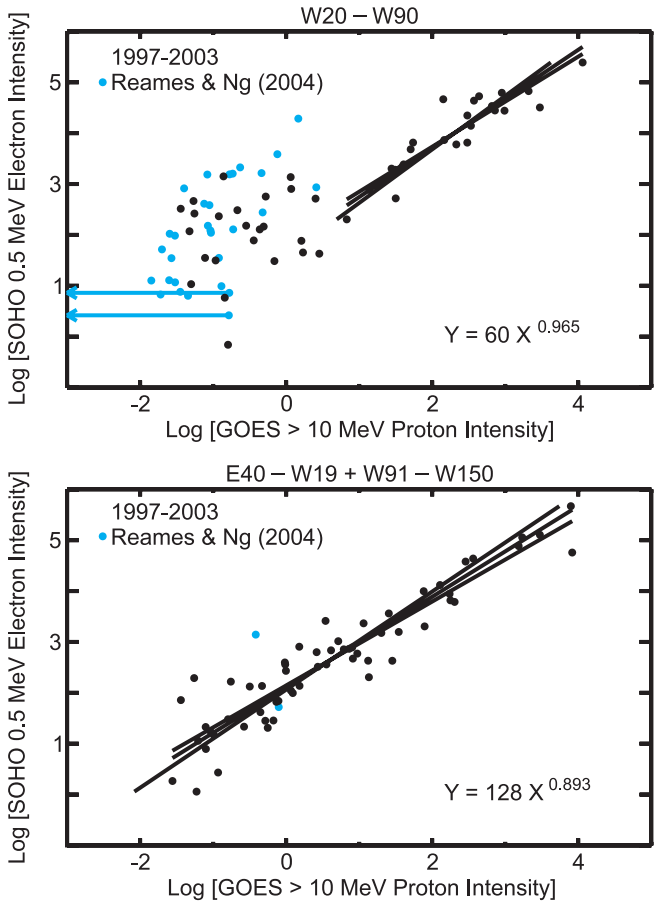

FIG. 2.—*Top*: Plot of peak 0.5 MeV electron intensity vs. peak >10 MeV proton intensity for well-connected (W20°–W90°) SEP events from 1997 January to 2004 April (from Table 1). The filled blue circles indicate the intense impulsive SEP events of Reames & Ng (2004). The least-squares fit is for events with peak >10 MeV intensities >3 protons cm^{-2} s^{-1} sr^{-1}. *Bottom*: Same as top, except for poorly connected (E40°–W19° and W91°–W150°) SEP events. In this case the least-squares fit is over the full range of data.

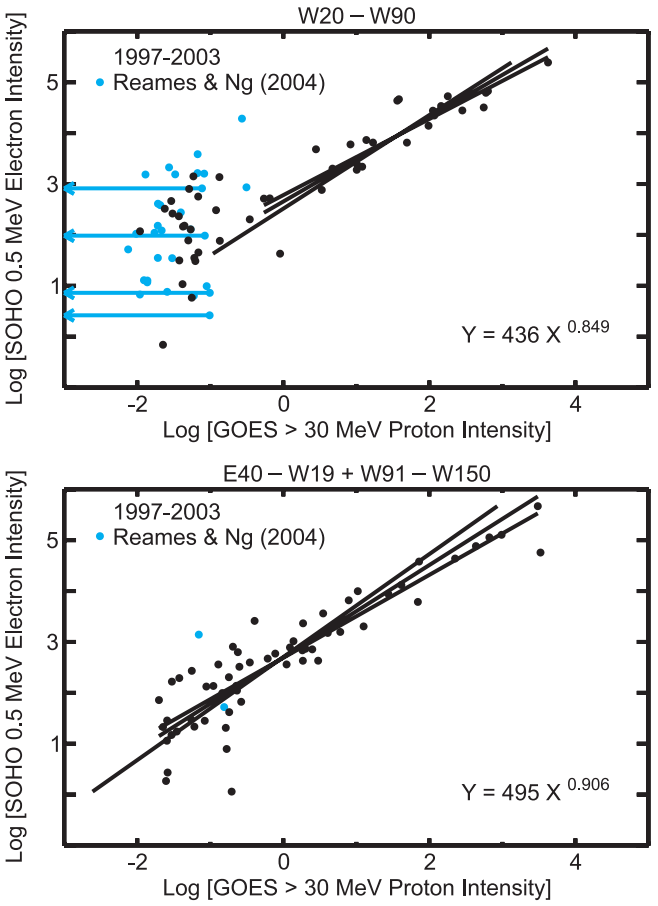

FIG. 3.—*Top*: Plot of peak 0.5 MeV electron intensity vs. peak >30 MeV proton intensity for well-connected (W20°–W90°) SEP events from 1997 January to 2004 April (from Table 1). The filled blue circles indicate the intense impulsive SEP events of Reames & Ng (2004). The least-squares fit is for events with peak >30 MeV intensities >0.5 protons cm^{-2} s^{-1} sr^{-1}. *Bottom*: Same as top, except for poorly connected (E40°–W19° and W91°–W150°) SEP events. In this case the least-squares fit is over the full range of data.

events of Reames & Ng (2004; *filled blue circles*) and an additional nine low-intensity (<3 particles) events[7] from Cane et al. (2002) with *e*/*p* ratios >1000 in Figure 2 (*top*) yields a ~20% (8/38; *Wind* WAVES data gap for one event) association rate, versus ~90% (23/25) for events with peak >10 MeV intensities >3 protons cm^{-2} s^{-1} sr^{-1}.

In Figure 2 (*bottom*) we plot 0.5 MeV peak electron intensities versus >10 MeV peak proton intensities for poorly connected events in Table 1, extending up to 60° on either side from the nominal W20°–W90° zone of good magnetic connection. Note that (1) small proton events with high *e*/*p* ratios (population 1) are largely missing from the figure;[8] and (2) the least-squares relationship shown in the figure, based in this case on the entire range of data, is similar to that derived for the events in Figure 2 (*top*) for population 2 events. Item (1) supports the view that the population 1 events are generated in flares, because small "cones of emission" are a commonly accepted characteristic of the flare particle acceleration process (e.g., Lin 1970b). More importantly, item (2) indicates that the same acceleration process responsible for the population 2 events from the well-connected zone (Fig. 2, *top*) can produce similar events when the responsible solar eruptions are well removed from W55°. Such behavior, bolstered by the high rate of DH type II radio association for front-side population 2 events, strongly suggests a shock mechanism. The DH association rate for front-side (E40°–W19°) events in Figure 2 (*bottom*) is 85% (23/27).

The continuation of the population 2 events down to the lowest peak intensities in Figure 2 (*bottom*) indicates that the low-intensity proton events in Figure 2 (*top*) are not a clean sample but include both flare events and shock-dominated events. A similar overlap in the two populations for small proton events can be surmised from Figure 1.

In Figure 2 the data points for the seven events, noted in § 2.1.2, for which the >10 MeV proton intensities peaked outside of the ~12 hr window fell within the general scatter of the points in the population 2 branch(es). Thus, we retained these seven events for Figure 2 and for the analyses described below.

2.2.2. 0.5 MeV *Electrons and* >30 MeV *Protons*

To check the hypothesis of Cane et al. (2003) that the flare particle acceleration process is generally dominant at ion energies >25 MeV $nucleon^{-1}$, we made plots of 0.5 MeV electron versus >30 MeV proton intensities for the well-connected (Fig. 3, *top*)

[7] D. Reames (2006, private communication) examined composition data for these nine candidate impulsive events and concluded that five had enhanced Fe/O and/or $^3He/^4He$ ratios; the other four cases were indeterminate because of low ion intensities.

[8] Of the events in Fig. 2 (*top*), 33% (26/79) have peak >10 MeV intensities <3 protons cm^{-2} s^{-1} sr^{-1} and *e*/*p* ratios >1000. The corresponding percentage for Fig. 2 (*bottom*) is 5% (3/61).

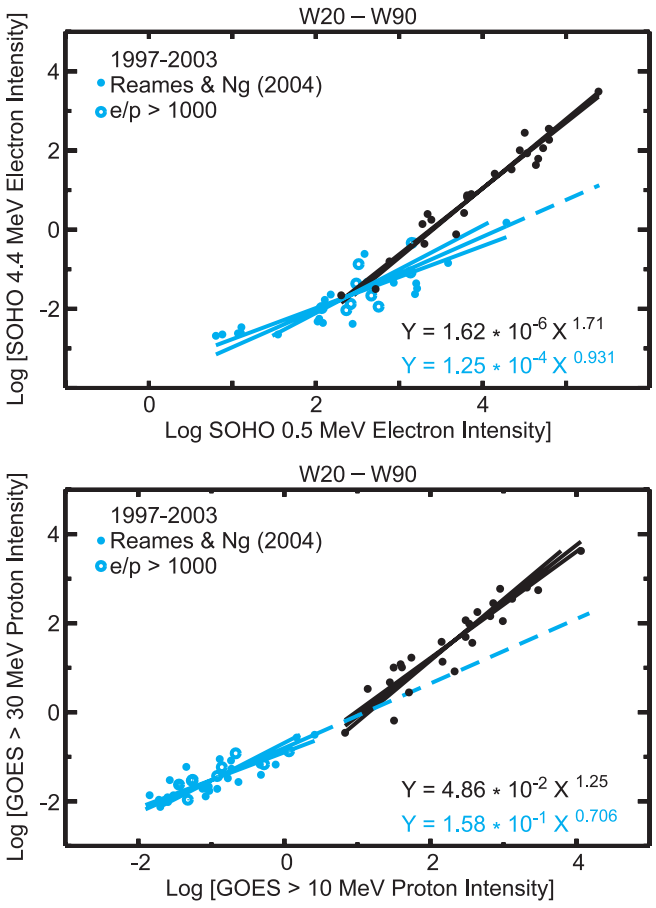

FIG. 4.—*Top*: Scatter plot of *SOHO* >4.4 MeV peak electron intensities vs. 0.5 MeV peak electron intensities for well-connected events from 1997 January to 2004 April (see text). Regression lines are drawn for both the population 1 (*blue*) and population 2 (*black*) events. *Bottom*: Scatter plot of *GOES* >30 MeV peak proton intensities vs. >10 MeV peak proton intensities for well-connected events from 1997 January to 2004 April. Regression lines are drawn for both the population 1 (*blue*) and population 2 (*black*) events. In both panels, events with upper limit intensities for either or both species are not plotted.

and poorly connected (Fig. 3, *bottom*) events in Table 1. The results are analogous to those in Figure 2: (1) evidence for two distinct populations in Figure 3 (*top*) with the low-intensity population characterized by a broad range of *e*/*p* ratios, (2) similar correlations between electron and proton intensities for large events in Figure 2 (*top*) and all events in Figure 3 (*bottom*), and (3) the absence of the population with high *e*/*p* ratios and trans-Fe enhancements in Figure 3 (*bottom*). The interpretation of Figure 3 in terms of two distinct populations, the first dominated by the flare and the second, comprising the most intense >30 MeV proton events, by the shock, is the same as that for Figure 2.

2.3. *Spectra of Flare and Shock SEP Events*

As a further test of the hypothesis that flare particles dominate SEP events at high energies, we considered SEP event spectra. Figure 4 (*top*) is a scatter plot of peak intensities of *SOHO* 4.4 MeV electrons versus peak intensities of 0.5 MeV electrons for groups of well-connected population 1 and population 2 events. (In both panels of Fig. 4, events with upper limits are not shown.) Regression lines are shown for both population 1 (taken here to consist of the impulsive events of Reames & Ng [2004, *filled blue circles*] and nine "black circle" events in Figure 2 [*top*], with *e*/*p* ratios >10^3; *open blue circles*) and population 2 (unambiguous events with >10 MeV peak intensities >3 protons; *black data points*) events. The least-squares fit for the population 1 events (*blue lines*) falls below that for the large population 2 events (*black lines*), indicating a steeper spectrum for electron events from flares than those attributed to shocks. Figure 4 (*bottom*) contains a scatter plot of *GOES* >30 MeV peak proton intensities versus >10 MeV peak proton intensities for the well-connected events in our sample. As in Figure 4 (*top*), we find evidence for steeper spectra for population 1 events than for large population 2 events. The regression line for the population 1 events, extrapolated to the highest >10 MeV intensity (10^4 protons) observed for a population 2 event, yields a peak >30 MeV intensity more than an order of magnitude (a factor of 46) smaller. For an independent check on this result, we constructed a similar plot (not shown) based directly and only on *ACE* data (i.e., not converted to *GOES* equivalent values via eqs. [2] and [3]). For this plot, the factor of 46 reduces to 17, a reflection of the uncertainty involved in determining the peak intensities (above background) of small population 1 events, and extrapolation of small differences in slope over more than 3 orders of magnitude. Note that these inferred differences by factors of 10 or more involve the assumption (in order to extrapolate the blue line) that a factor of ~100 increase in flare size (the difference in integrated 1–8 Å intensity between the largest flares associated with population 1 and population 2 events; § 2.2.1) can produce a factor of ~10,000 increase in >10 MeV proton intensity. Since the >10 MeV intensity increases more slowly with flare size (see, e.g., Belov et al. 2005), the inferred contributions from flares to the largest SEP events at 30 MeV (Fig. 4, *bottom*) are likely overstated.

3. SUMMARY AND DISCUSSION

Ramaty et al. (1980) interpreted Figure 1 in terms of two basic particle acceleration processes at the Sun: a flare process responsible for SEP events with low peak proton intensities and high *e*/*p* ratios, and a higher energy process, presumably shock related, that accounted for intense proton events. By using a larger data set spanning a broader range of longitudes, and considering higher SEP energies, we have replicated/substantiated the result of Ramaty et al.

In Figures 2 and 3 (*top panels*), the large proportion of intense impulsive SEP events from the list of Reames & Ng (2004) in the group of low-intensity proton events with high *e*/*p* ratios (population 1) supports the attribution by Ramaty et al. (1980) of these events to a flare acceleration process, as does their weak association with DH type II radio busts. In Figures 2 and 3 (*bottom panels*) the relative absence of events with high *e*/*p* ratios from poorly connected sources reinforces the identification of the so-called population 1 events with the particle acceleration process resident in flares because of the small cone of emission for flare SEP events (e.g., Lin 1970b; Nitta et al. 2006).

The correlation of peak 0.5 MeV electrons and >10/>30 MeV proton intensities over 5 orders of magnitude in Figures 2 and 3 (*bottom panels*) suggests a common acceleration process for these species in population 2 events. In addition, the similarity of the population 2 branches in the top and bottom panels of Figures 2 and 3 indicates an acceleration process capable of operating over a wide range of longitudes. Coupled with the strong association of the population 2 events with DH type II bursts (Gopalswamy et al. 2002; Cliver et al. 2004), this last observation argues that shock acceleration is the dominant mechanism operating in intense proton events, at least to energies ~30 MeV.

The spectral evidence in Figure 4 indicates that this dominance extends to higher energies. The steeper proton spectra for

population 1 events imply that the flare contribution to the largest proton events at ~30 MeV is at least an order of magnitude smaller than the shock contribution. Thus, we do not find support for the contention of Cane et al. (2003) that >25 MeV nucleon^{-1} ions originate preferentially in the flare particle acceleration process (or processes).

Recently, Tylka et al. (2005) and Tylka & Lee (2006) have presented evidence that compositional differences observed for heavy ions in intense (population 2) SEP events can be explained in terms of shock acceleration when one takes shock geometry and seed particles into account. Here, we have argued that a coronal/interplanetary shock is also the principal accelerator for electrons and protons, the major constituents, in large SEP events.

We thank Steve Kahler and Allan Tylka for comments on a draft of this paper and acknowledge helpful discussions with Bill Dietrich, Nariaki Nitta, and Don Reames. We thank Arik Posner and Andreas Klassen for assistance with the *SOHO* electron data, and the *ACE* SIS team, the *ACE* EPAM team, and the *ACE* Science Center for providing the *ACE* data. A. G. L. was supported by AFRL contract FA8718-05-C-0036.

REFERENCES

Belov, A., Garcia, H., Kurt, V., Mavromichalaki, H., & Gerontidou, M. 2005, Sol. Phys., 229, 135, DOI: 10.1007/s11207-005-4721
Bougeret, J.-L., et al. 1995, Space Sci. Rev., 71, 231
Breneman, H. H., & Stone, E. C. 1985, ApJ, 299, L57
Cane, H. V., Erickson, W. C., & Prestage, N. P. 2002, J. Geophys. Res., 107, 1315, DOI: 10.1029/2001JA000320
Cane, H. V., McGuire, R. E., & von Rosenvinge, T. T. 1986, ApJ, 301, 448
Cane, H. V., Mewaldt, R. A., Cohen, C. M. S., & von Rosenvinge, T. T. 2006, J. Geophys. Res., 111, A06590, DOI: 10.1029/2005JA011071
Cane, H. V., von Rosenvinge, T. T., Cohen, C. M. S., & Mewaldt, R. A. 2003, Geophys. Res. Lett., 30, 8017, DOI: 10.1029/2002GL016580
Cliver, E. W., Kahler, S. W., & Reames, D. V. 2004, ApJ, 605, 902
Gold, R. E., et al. 1998, Space Sci. Rev., 86, 541
Gopalswamy, N., et al. 2002, ApJ, 572, L103
Klecker, B., Hovestadt, D., Scholer, M., Gloeckler, G., Ipavich, F. M., Fan, C. Y., & Fisk, L. A. 1984, ApJ, 281, 458
Leske, R. A., Wiedenbeck, M. E., Cohen, C. M. S., Mewaldt, R. A., Cummings, A. C., Stone, E. C., & von Rosenvinge, T. T. 2003, Proc. 28th Int. Cosmic-Ray Conf. (Tsukuba), 3253
Lin, R. P. 1970a, Sol. Phys., 12, 266
———. 1970b, Sol. Phys., 15, 453
Lin, R. P., & Anderson, K. A. 1967, Sol. Phys., 1, 446
Lin, R. P., & Hudson, H. S. 1976, Sol. Phys., 50, 153
Lin, R. P., Mewaldt, R. A., & Van Hollebeke, M. A. I. 1982, ApJ, 253, 949
Mason, G. M., Mazur, J. E., Dwyer, J. R., Jokipii, J. R., Gold, R. E., & Krimigis, S. M. 2004, ApJ, 606, 555
Mason, G. M., Reames, D. V., von Rosenvinge, T. T., Klecker, B., & Hovestadt, D. 1986, ApJ, 303, 849
Müller-Mellin, R., et al. 1995, Sol. Phys., 162, 483
Nitta, N. V., Reames, D. V., DeRosa, M. L., Liu, Y., Yashiro, S., & Gopalswamy, N. 2006, ApJ, 650, 438
Ramaty, R., et al. 1980, in Solar Flares, ed. P. A. Sturrock (Boulder: Colorado Associated Univ. Press), 117
Reames, D. V. 1999, Space Sci. Rev., 90, 413
———. 2000, ApJ, 540, L111
Reames, D. V., & Ng, C. K. 2004, ApJ, 610, 510
Reames, D. V., Stone, R. G., & Kallenrode, M.-B. 1991, ApJ, 380, 287
Reames, D. V., von Rosenvinge, T. T., & Lin, R. P. 1985, ApJ, 292, 716
Stone, E. C., et al. 1998, Space Sci. Rev., 86, 357
Tylka, A. J., & Lee, M. A. 2006, ApJ, 646, 1319
Tylka, A. J., et al. 2005, ApJ, 625, 474
Van Hollebeke, M. A. I., Ma Sung, L. S., & McDonald, F. B. 1975, Sol. Phys., 41, 189
von Rosenvinge, T. T., et al. 1995, Space Sci. Rev., 71, 155
Wang, Y.-M., Pick, M., & Mason, G. M. 2006, ApJ, 639, 495
Wild, J. P., Smerd, S. F., & Weiss, A. A. 1963, ARA&A, 1, 291